Modeling and Characterization of Transmission Energy Consumption in Machine-to-Machine Networks

M. G. Khoshkholgh*, Y. Zhang***, K. G. Shin**, V. C. M. Leung*, S. Gjessing***
* Department of Electrical and Computer Engineering, the University of British Columbia
** Department of Electrical and Computer Science, the University of Michigan
***Simula Research Laboratory, Fornebu, Norway

***Abstract*—In future, a massive number of devices are expected to communicate for pervasive monitoring and measurement, industrial automation, and home/building energy management. Nevertheless, such Machine-to-Machine (M2M) communications are prone to failure due to depletion of machines energy if the communication system is not designed properly. A key step in building energy-efficient protocols for large-scale M2M communications is to assess, model or characterize a *network energy consumption profile*. To meet this need, we develop a theoretical and numerical framework to evaluate the cumulative distribution function (CDF) of the total energy consumption by fully exploiting the properties of stochastic geometry. Unlike the other existing approaches, we model the transmission energy as a function of transmission power, packet size, and link affordable capacity that is a logarithmic function of experienced Signal to Interference plus Noise Ratio (SINR). Since it is very difficult, if not impossible, to derive a closed-form expression for the CDF, we derive numerically computable first- and second-order moments of energy consumption. Applying these moments we then propose Log-normal and Log-logistic distributions to approximate the CDF. Our simulation results show that Log-logistic almost precisely approximates the exact CDF.**

I. Introduction

Numerous applications, such as remote e-health, smart home, smart power grid, environmental monitoring, and industrial automation need ubiquitous sensing, widespread data sharing and decisions, and human-free intervention [1], [2]. Managing wireless access by a massive number of machines to meet a variety of QoS requirements including reliability, security, latency, and energy consumption is one of the main challenges in M2M networks [3], [4]. In this paper we aim to characterize the energy consumption in a large M2M network.

Energy-based access control and resource allocation were studied in [3]. However, only a single cell was considered there. The authors of [5] introduced a new performance metric called *bandwidth-distance product* to analyze the scalability of a hierarchical cyber-physical system. To facilitate communications, aggregation nodes (ANs) – acting as data collectors and perhaps compressors [6], [7] – are devised and deployed to gather and process measurements before relaying to higher hierarchical components [8]. *Random deployment* of ANs is known to be effective and practical in designing (Machine-to-Machine) M2M networks, and also to provide reliable data communication links [8], [9]. Signal to Interference plus Noise Ratio (SINR) distribution and coverage analysis are the main subjects of [8], [9] where the properties of stochastic geometry and Poisson Point Process (PPP) [10] are used.

As in [8], [9], we also use stochastic geometry for our analysis due mainly to its flexibility in providing a holistic approach for modeling the network, and its mathematical amenability for analyzing the network's vital performance metrics [11]. However, instead of coverage analysis focused in [8], [9] our main goal here is on modeling and characterizing the energy consumption in large-scale M2M communications. The main motivations behind this investigation are: (i) M2M traffic is basically comprised of a huge number of short sessions, in spite of long duration sessions in human-driven traffic [12], and hence the capacity may not be a prime concern; (ii) Devices in machine-type communications are battery-limited and in many cases it is technically and economically difficult to recharge/replace the batteries; (iii) Green aspects of future wireless communications are becoming part of the objectives in engineering and optimization [1], [13]. However, according to our best knowledge comprehensive assessment of the energy consumption profile in a large-scale M2M communications has not been done before. Futuristic network planning is objectively entangled with energy efficiency, and the results of this investigation will help establish systematic guidelines for design of energy-efficient protocols. Furthermore, in scheduling and allocating resources, we need to consider inherent/engineered limitations on the network energy consumption profile as in current practices with capacity-driven objectives using the coverage performance profile.

This paper makes the following contributions. By exploiting stochastic geometry, we model and analyze the energy consumed in each cell. The transmission energy captures the capacity, transmission power and packet size. Laplace transform and moments of the accumulated interference are further computed. The CDF of the total consumed energy in each cell is theoretically evaluated by deriving the Laplace transform and a lower bound. We further consider use of a log-normal and log-logistic distributions to approximate the CDF of the consumed energy. Our simulation studies reveal that log-normal approximations have acceptable accuracy and follows the trend of the actual CDF. Furthermore, log-logistic in general outperforms log-normal approximation, and almost precisely fits the actual trends seen in simulations. Thus, one may draw a conclusion that the network energy consumption profile is Log-logistically distributed.

978-1-4799-8406-0/15/$31.00 ©2015 IEEE

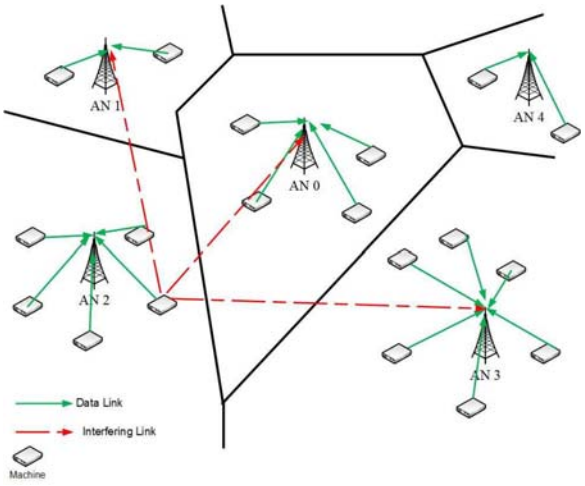

Fig. 1. A typical M2M communications network consisting of a massive number of machines and randomly deployed aggregation nodes

II. Energy Consumption in M2M Networks

Fig. 1 shows a schematic of the considered system model in this paper. A M2M network consists of aggregation nodes (ANs) and machines, both randomly scattered in the coverage area. In such a topology, ANs form a homogenous PPP (HPPP) Φ_1 with density λ_1. Similarly, machines belong to an HPPP Φ_0 independently of Φ_1 with density λ_0. We use subscripts i and j to respectively refer to the i-th machine and the j-th AN. Machines send the measured/sensed data to the closest AN. Accordingly, the concept of the cell in our system model is based on the geographical proximity, i.e., the cell associated with AN j consists of the all machines associated with it.

We consider a wireless communication session of total bandwidth ω Hz that is divided into W flat fading sub-channels, each with a bandwidth smaller than the channel's coherence bandwidth. Let τ be the frame duration that is divided into T equal parts, each of which is referred to as a *time slot*. Each machine should transmit data to its serving AN on a designated sub-channel and during a time slot.

The transmission energy is a function of data rate, power, and packet size. Here we do not consider the drain efficiency of the transmitter, energy of the sleeping mode, and the energy consumed by processing components. But, this is generally straightforward to incorporate these sources of energy consumption (at least via appropriate approximations) into the model. The data rate is a function of transmission power, distance between sender and receiver, and noise power as well as inter-cell interference, and is determined by the Signal-to-Interference-plus-Noise Ratio (SINR). Let AN j receive data from machine i, then SINR is given by

$$\mathrm{SINR}_{ij} = P_0 \frac{D(\|X_i - Y_j\|)H_{ij}}{n + I_j(w,t)}, \tag{1}$$

where n is an AWGN with power σ^2. All machines transmit packets with fixed power P_0. Distance-dependent path-loss attenuation is modeled as $D(\|X_i - Y_j\|) = \min\{1, \|X_i - Y_j\|^{-\alpha}\}$ where $\alpha > 2$ is the path-loss exponent and $\|X_i - Y_j\|$ is the Euclidian distance between machine i located at X_i and AN j located at Y_j. Note that to prevent power amplification for distances less than 1 meter, we used minimum operation. H_{ij} is the channel power gain between machine i and AN j that is in general location-independent and drawn from a common pdf $f_H(.)$. Let $\Phi_j(w,t)$ be a set of machines that transmit data on sub-channel w in time slot t. Also, let $\tilde{\Phi}_j$ denote a set of other-cell machines transmitting on sub-channel w in time slot t as $\tilde{\Phi}_j(w,t) = \left\{i \in \Phi_0(w,t) \bigcap \mathbb{V}_j^c(\Phi_1)\right\}$, where $\mathbb{V}_j(\Phi_1)$ is the Voronoi cell induced by AN j and $\mathbb{V}_j^c(\Phi_1)$ is the complementary set of $\mathbb{V}_j(\Phi_1)$. Note that only $1/TW$ of all machines outside $\mathbb{V}_j(\Phi_1)$ use the same time slot and sub-channel as machine i in $\mathbb{V}_j(\Phi_1)$. This is valid since ANs assign time slots and sub-channels independently. $I_j(w,t)$, the accumulated interference from machines transmitting in neighbor cells, i.e., $\{i \in \Phi_0 \bigcap \mathbb{V}_j^c(\Phi_1)\}$, on sub-channel w in time slot t, is then formulated as

$$I_j(w,t) = \sum_{i' \in \tilde{\Phi}_j(w,t)} P_0 D(\|X_{i'} - Y_j\|)\tilde{H}_{i'j},$$

where $\tilde{H}_{i'j}$ independent of H_{ij} for $i \in \mathbb{V}_j(\Phi_1)$ is the channel power gain between machine i' and the AN j that is drawn from the pdf $f_H(.)$. The capacity link in bits per second between machine i and AN j can be obtained from the Shannon formula

$$C_{ij} = \frac{\omega}{W} \log\left(1 + \mathrm{SINR}_{ij}\right).$$

Each machine has a packet of B bits to transmit to AN j on the link with capacity C_{ij}. Transmission energy, E_{ij}, is then the product of transmission power P_0 and transmission time $\frac{B}{C_{ij}}$:

$$E_{ij} = \frac{P_0 B}{\frac{\omega}{W} \log\left(1 + \mathrm{SINR}_{ij}\right)}. \tag{2}$$

Let Σ_j denote the overall energy consumed by the machines served by AN j which is, in general, a random variable. In this paper, we want to characterize this random variable by approximating its cumulative distribution function (CDF) or complementary CDF (CCDF). We first model the interference in M2M communications.

III. Interference Modeling

Due to the stationarity of PPPs, we only need to focus on the statistics of interference at the origin, $I_0(w,t)$. In the following Proposition, we derive the Laplace transform $\mathcal{L}_{I_0(w,t)}(s)$.

Proposition 1: The Laplace transform of a random variable $I_0(w,t)$, $\mathcal{L}_{I_0(w,t)}(s)$, is

$$= \sum_{n=0}^{\infty} \frac{(-\lambda_0/TW)^n}{n!} \int_{\mathbb{R}^2} \cdots \int_{\mathbb{R}^2} \prod_{m=1}^{n} [1 - \mathbb{E}_{\tilde{H}} e^{-sP_0 D(\|x_m\|)\tilde{H}}] dx_m$$
$$\times \left[1 - \sum_{m=1}^{n} (-1)^{m+1} \sum_{1 \le l_1 \le l_2 \le \ldots \le l_m \le n} e^{-\lambda_1 S(x_{l_1}, x_{l_2}, \ldots, x_{l_m})}\right],$$

where $S(x_{l_1}, x_{l_2}, \ldots, x_{l_m})$ is the area of union section of m disks located at x_{l_m} with the corresponding radius $\|x_{l_m}\|$.

Proof: By definition, the Laplace transform of the random variable $I_0(w,t)$ is

$$\mathcal{L}_{I_0(w,t)}(s) \quad = \quad \mathbb{E} \prod_{i\in\tilde{\Phi}_0(w,t)} \mathbb{E}_{\tilde{H}_i} e^{-sP_0 D(\|X_i\|)\tilde{H}_i}, \quad (3)$$

in which we used the independence of the fading fluctuations at different locations. Adopting Campbell's Theorem, we get

$$\mathcal{L}_{I_0(w,t)}(s) = \mathbb{E}_1^0 e^{-\frac{\lambda_0}{TW}\int\limits_{\mathbb{V}_0^c(\Phi_1)}[1-\mathbb{E}_{\tilde{H}}e^{-sP_0D(\|x\|)\tilde{H}}]dx}$$

$$= \mathbb{E}_1^0 \sum_{n=0}^{\infty} \frac{(-\frac{\lambda_0}{TW})^n}{n!} \left(\int\limits_{\mathbb{V}_0^c(\Phi_1)} [1-\mathbb{E}_{\tilde{H}}e^{-sP_0D(\|x\|)\tilde{H}}]dx \right)^n$$

$$= \sum_{n=0}^{\infty} \frac{(-\frac{\lambda_0}{TW})^n}{n!} \mathbb{E}_1^0 \int\limits_{\mathbb{V}_0^c(\Phi_1)} \cdots \int\limits_{\mathbb{V}_0^c(\Phi_1)} \times \prod_{m=1}^{n} [1-\mathbb{E}_{\tilde{H}}e^{-sP_0D(\|x_m\|)\tilde{H}}]dx_1 \ldots dx_n$$

$$= \sum_{n=0}^{\infty} \frac{(-\frac{\lambda_0}{TW})^n}{n!} \mathbb{E}_1^0 \int\limits_{\mathbb{R}^2} \cdots \int\limits_{\mathbb{R}^2} \prod_{m=1}^{n} [1-\mathbb{E}_{\tilde{H}}e^{-sP_0D(\|x_m\|)\tilde{H}}] \times 1_{\{(x_1,\ldots,x_m)\in\mathbb{V}_0^c(\Phi_1)\}} dx_1 \ldots dx_n$$

$$= \sum_{n=0}^{\infty} \frac{(-\frac{\lambda_0}{TW})^n}{n!} \int\limits_{\mathbb{R}^2} \cdots \int\limits_{\mathbb{R}^2} \prod_{m=1}^{n} [1-\mathbb{E}_{\tilde{H}}e^{-sP_0D(\|x_m\|)\tilde{H}}] \times \mathbb{P}\{(x_1,\ldots,x_m)\in\mathbb{V}_0^c(\Phi_1)\}dx_1 \ldots dx_n$$

$$= \sum_{n=0}^{\infty} \frac{(-\frac{\lambda_0}{TW})^n}{n!} \int\limits_{\mathbb{R}^2} \cdots \int\limits_{\mathbb{R}^2} \prod_{m=1}^{n} [1-\mathbb{E}_{\tilde{H}}e^{-sP_0D(\|x_m\|)\tilde{H}}] \times \left[1-\mathbb{P}\left\{\bigcup_{m=1}^{n} x_m \in \mathbb{V}_0(\Phi_1)\right\}\right] dx_1 \ldots dx_n, \quad (4)$$

where in the last step we applied Demorga's law. Here $\mathbb{E}_1^0$ denotes the expectation with respect to the Palm distribution of the point process Φ_1. Note that from the rule of the union probability, we get

$$\mathbb{P}\left\{\bigcup_{m=1}^{n} x_m \in \mathbb{V}_0(\Phi_1)\right\} \quad = \quad \sum_{m=1}^{n}(-1)^{m+1} \sum_{1\le l_1\le l_2\le\ldots\le l_m\le n} \times \mathbb{P}\left\{(x_{l_1},x_{l_2},\ldots,x_{l_m})\in\mathbb{V}_0(\Phi_1)\right\}, \quad (5)$$

in which

$$\mathbb{P}\left\{(x_{l_1},x_{l_2},\ldots,x_{l_m})\in\mathbb{V}_0(\Phi_1)\right\} = e^{-\lambda_1 S(x_{l_1},x_{l_2},\ldots,x_{l_m})} \quad (6)$$

where $S(x_{l_1},x_{l_2},\ldots,x_{l_m})$ is the area of unioned section of m disks located at x_{l_m} with the corresponding radius $\|x_{l_m}\|$. By substituting (6) into (5) and inserting the result in (4), the desired result follows. Q.E.D.

Though Laplace transform entirely characterizes the statistical behavior of the interference in the network, unfortunately, Proposition 1 may not yield a numerically computable integral form. Consequently, an alternative approach is needed to appropriately approximate the impact of interference on energy consumption. A widely accepted and sufficiently accurate approach is to approximate the true pdf using moments of the random variable $I_0(w,t)$. For the case of Rayleigh fading, our simulation results are plotted in Fig. 2. The histogram is shown to have heavy-tailed skews. In this figure, we also added fitted Gaussian and log-normal distributions. The log-normal distribution is shown to be able to capture these two phenomena, and hence it is used for approximating the interference. To apply the Log-Normal approximation, we need to evaluate the first and second cumulants of the interference. The first-order cumulant, β_1, is

$$\beta_1 \quad = \quad P_0 \frac{\lambda_0}{TW} \int\limits_{\mathbb{R}^2} D(\|x\|)\mathbb{P}\left\{x\in\mathbb{V}_0^c(\Phi_1)\right\} dx, \quad (7)$$

where $\mathbb{P}\left\{x\in\mathbb{V}_0^c(\Phi_1)\right\} = 1-e^{-\pi\lambda_1\|x\|^2}$. The second-order cumulant or variance is obtained as

$$\beta_2 \quad = \quad \mathbb{E} \sum_{i,i'\in\tilde{\Phi}_0(w,t)}^{\neq} P_0^2 \tilde{H}_i \tilde{H}_{i'} D(\|X_i\|)D(\|X_{i'}\|) \quad (8)$$

$$+ \quad \mathbb{E} \sum_{i\in\tilde{\Phi}_0(w,t)} P_0^2 D^2(\|X_i\|)\tilde{H}_i^2 - (\beta_1)^2. \quad (9)$$

It is then straightforward to verify

$$(9) = P_0^2 \mathbb{E}H^2 \frac{\lambda_0}{TW} \int\limits_{\mathbb{R}^2} D^2(\|x\|)\left(1-e^{-\pi\lambda_1\|x\|^2}\right)dx - (\beta_1)^2.$$

Furthermore,

$$(8) \quad = \quad P_0^2 \left(\frac{\lambda_0}{TW}\right)^2 \int\limits_{\mathbb{R}^2}\int\limits_{\mathbb{R}^2} D(\|x\|)D(\|x'\|) \times \mathbb{P}\left\{(x,x')\in\mathbb{V}_0^c(\Phi_1)\right\} dxdx'. \quad (10)$$

where the term $\mathbb{P}\left\{(x,x')\in\mathbb{V}_0^c(\Phi_1)\right\}$ can be evaluated via Demorga's law as:

$$\mathbb{P}\left\{(x,x')\in\mathbb{V}_0^c(\Phi_1)\right\} \quad = \quad 1-\mathbb{P}\left\{x\in\mathbb{V}_0(\Phi_1)\right\} - \mathbb{P}\left\{x'\in\mathbb{V}_0(\Phi_1)\right\} + \mathbb{P}\left\{(x,x')\in\mathbb{V}_0(\Phi_1)\right\}. \quad (11)$$

Substituting this in (10), (8) becomes

$$= \left(P_0\frac{\lambda_0}{TW}\int\limits_{\mathbb{R}^2} D(\|x\|)dx\right)^2$$

$$- \quad 2P_0^2\left(\frac{\lambda_0}{TW}\right)^2 \int\limits_{\mathbb{R}^2} D(\|x\|)e^{-\pi\lambda_1\|x\|^2}dx \int\limits_{\mathbb{R}^2} D(\|x'\|)dx'$$

$$+ \quad P_0^2\left(\frac{\lambda_0}{TW}\right)^2 \int\limits_{\mathbb{R}^2}\int\limits_{\mathbb{R}^2} D(\|x\|)D(\|x'\|) \times \mathbb{P}\left\{(x,x')\in\mathbb{V}_0(\Phi_1)\right\} dxdx'. \quad (12)$$

It is then possible to apply [14] to calculate the above quantity.

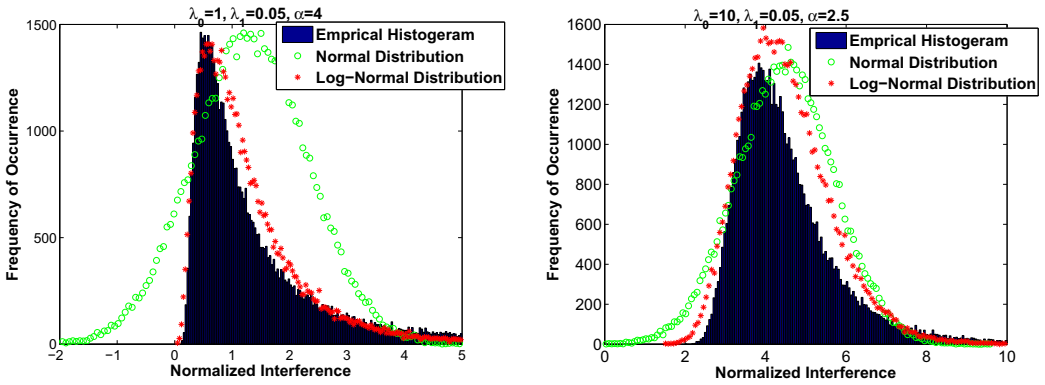

Fig. 2. Empirical histogram of the experienced accumulated interference.

IV. CDF of Transmission Energy Consumption

We now evaluate the CDF of the total consumed energy in a cell. For this goal we first derive the Laplace transform of the total consumed energy at the typical cell. The following proposition suggests an expression for its Laplace transform.

Proposition 2: $\mathcal{L}_{\Sigma_0}(s)$ is

$$\mathcal{L}_{\Sigma_0}(s) = \sum_{n=0}^{\infty} \frac{(-\lambda_0)^n}{n!} \int_{\mathbb{R}^2} \cdots \int_{\mathbb{R}^2} e^{-\lambda_1 S(x_1,x_2,\ldots,x_n)} \times \prod_{m=1}^{n} [1 - \mathbb{E}_H \mathbb{E}_I e^{-s \frac{P_0 B}{\frac{\omega}{W} \log\left(1+P_0 \frac{D(\|x_m\|)H}{\sigma^2+I}\right)}}] dx_m.$$

Proof: One may show that the Laplace transform of Σ_0 is

$$\mathcal{L}_{\Sigma_0}(s) = \mathbb{E}_1^0 e^{-\lambda_0 \int\limits_{\mathbb{V}_0(\Phi_1)} [1-\mathbb{E}_H \mathbb{E}_I e^{-s \frac{P_0 B}{\frac{\omega}{W} \log(1+\mathrm{SINR}_x)}}] dx} \quad (13)$$

We then need to follow the lines in the proof of Proposition 1 to prove the proposition statement. Q.E.D.

Note that again it seems impossible to derive a closed-form expression for the Laplace transform, thus making the evaluation of the CDF very challenging. An alternative might be to derive a lower-bound of the CCDF. The following proposition provides a lower-bound of the CCDF of the transmission energy.

Proposition 3: A lower-bound on CCDF of the transmission energy may be

$$\mathbb{P}\{\Sigma_0 > x\} \geq \sum_{n=1}^{\infty} (-1)^{n+1} \frac{(\lambda_0)^n}{n!} \int_{\mathbb{R}^2} \cdots \int_{\mathbb{R}^2} e^{-\lambda_1 S(x_1,x_2,\ldots,x_n)} \times \prod_{m=1}^{n} \mathbb{E}_I F_H \left(\frac{2^{\frac{BWP_0}{\mathrm{x}\omega}} - 1}{P_0} (\sigma^2 + I) D(\|x_m\|) \right) dx_m.$$

Proof: First, let's define set $\check{\Phi}_0$

$$\check{\Phi}_0(\mathrm{x}) = \left\{ i \in \Phi_0 / \tilde{\Phi}_0 : \frac{P_0 B}{\frac{\omega}{W} \log(1+\mathrm{SINR}_{i0})} > \mathrm{x} \right\}, \quad (14)$$

which contains those machines associated with AN 0 with energy consumption more than a given energy threshold x. A simple manipulation reveals that this set can also be expressed via the SIR requirement $\{\mathrm{SINR}_i < \rho(\mathrm{x})\}$ where $\rho(\mathrm{x})$ is defined as $\rho(\mathrm{x}) = 2^{\frac{BWP_0}{\mathrm{x}\omega}} - 1$. A lower-bound on CCDF is then suggested as

$$\mathbb{P}\left\{ \sum_{i \in \Phi_0 \bigcap \mathbb{V}_0(\Phi_1)} E_i > \mathrm{x} \right\} \geq 1 - \mathbb{P}\{\check{\Phi}_0(\mathrm{x}) = \emptyset\}, \quad (15)$$

or equivalently,

$$\mathbb{P}\{\Sigma_0 > \mathrm{x}\} \geq 1 - \mathbb{E} e^{-\lambda_0 \int\limits_{\mathbb{V}_0(\Phi_1)} \mathbb{P}\{\mathrm{SINR}_x < \rho(\mathrm{x})\} dx}, \quad (16)$$

which leads to the statement after applying Taylor expansion of the exponential function and following the lines in the proof of Proposition 1. Q.E.D.

On the other hand, evaluating this lower-bound is again rather complicated and may not end up with a closed-from expression. We therefore approximate the true CDF with some appropriate distributions. The log-normal distribution and log-logistic distribution are among the options we will consider with acceptable computational complexity.

Fig. 3 illustrates some simulation results on an empirical histogram of the consumed energy in a cell. This figure also shows the fitted log-logistic distribution. As shown in all cases, the log-logistic distribution provides a very accurate approximation, so we will henceforth assume that the actual CDF is log-logistic. It is thus necessary to derive the first and second moments as follows.

Let's start with $\mathbb{E}^0[\Sigma_0]$ which is equal to

$$= \mathbb{E} \sum_{i \in \Phi_0} \mathbf{1}\left(i \in \mathbb{V}_0(\Phi_1)\right) \times \mathbb{E}_{H_{i0}} \mathbb{E}_I \frac{P_0 B}{\frac{\omega}{W} \log\left(1 + P_0 \frac{D(\|X_i\|)H_{i0}}{\sigma^2+\beta_2}\right)}$$

$$= \lambda_0 P_0 \mathbb{E}_1^0 \int\limits_{\mathbb{V}_0(\Phi_1)} \mathbb{E}_H \mathbb{E}_I \frac{1}{\frac{\omega}{W} \log\left(1 + P_0 \frac{D(\|x\|)H}{\sigma^2+I}\right)} dx,$$

Noting the convexity of

$$\frac{1}{\frac{\omega}{W} \log\left(1 + P_0 \frac{D(\|x\|)H}{\sigma^2+I}\right)},$$

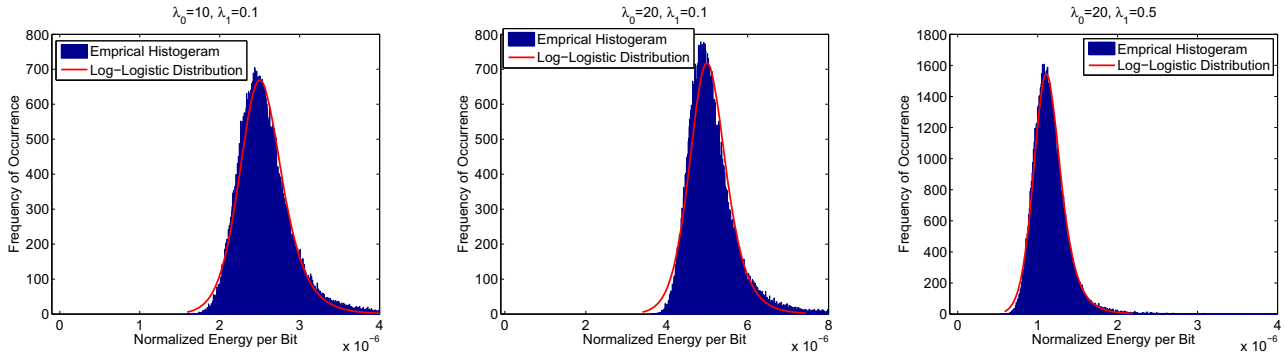

Fig. 3. Empirical histogram of the total consumed energy in a cell.

with respect to fading power gain, we derive a lower-bound $\mathbb{E}_1^0[\Sigma_0]$ as follows

$$\mathbb{E}_1^0[\Sigma_0] \geq \lambda_0 P_0 \mathbb{E}_1^0 \int\limits_{\mathbb{V}_0(\Phi_1)} \mathbb{E}_I \frac{1}{\frac{\omega}{W}\log\left(1+P_0\frac{D(\|x\|)\mathbb{E}_H H}{\sigma^2+I}\right)}dx$$

$$= \lambda_0 P_0 \mathbb{E}_1^0 \int\limits_{\mathbb{V}_0(\Phi_1)} \mathbb{E}_I \frac{1}{\frac{\omega}{W}\log\left(1+P_0\frac{D(\|x\|)}{\sigma^2+I}\right)}dx$$

$$= \lambda_0 P_0 B \int\limits_{\mathbb{R}^2} \mathbb{E}_I \frac{e^{-\pi\lambda_1\|x\|^2}}{\frac{\omega}{W}\log\left(1+P_0\frac{D(\|x\|)}{\sigma^2+I}\right)}dx.$$

This way $\mathbb{E}^0[\Sigma_0^2]$ may also be lower-bounded as

$$\geq \lambda_0 P_0^2 B^2 \mathbb{E}_1^0 \int\limits_{\mathbb{V}_0(\Phi_1)} \mathbb{E}_I \left(\frac{1}{\frac{\omega}{W}\log\left(1+P_0\frac{D(\|x\|)}{\sigma^2+I}\right)}\right)^2 dx$$

$$+\lambda_0^2 P_0^2 B^2 \mathbb{E}_1^0 \int\limits_{\mathbb{V}_0(\Phi_1)}\int\limits_{\mathbb{V}_0(\Phi_1)} \mathbb{E}_I \frac{\left(\frac{\omega}{W}\log\left(1+P_0\frac{D(\|x\|)}{\sigma^2+I}\right)\right)^{-1}}{\frac{\omega}{W}\log\left(1+P_0\frac{D(\|y\|)}{\sigma^2+I}\right)}dydx.$$

Having the moments, it is easy to provide an approximate CDF with the log-normal distribution.

Fig. 4 shows the CDF of Σ_0 for different densities of machines and ANs[1]. For comparison we also show the log-logistic approximation. The log-logistic distribution is shown to be a very accurate and follow the trends observed in the actual CDF. We also study the accuracy of log-normal approximation in Fig. 5. It is observed that the log-normal distribution is fairly accurate, particularly when λ_1/λ_0 is small enough. Increasing λ_1 reduces the accuracy of log-normal approximation as it cannot exactly capture the *phase transition* observed in the actual CDF. Note that this phase transition is more pronounced for large λ_1. Furthermore, by increasing the path-loss exponent α, the accuracy of log-normal approximation is also degraded. On the other hand, comparison of Fig. 4and Fig. 5 indicates that the log-logistic distribution is more accurate in approximating the true CDF than log-normal distribution.

[1]For simulation we set $W = 1028$, $\omega = 10$ MHz, $T = 20$ and $\sigma^2 = 10^{-12}$ Watts.

A. Discussions

One of the main applications of the findings of this paper can be the design of the M2M systems. In the following we provide a brief guideline for this goal. Assume the designer is interested in designing the network by selecting the best density of ANs. The optimization problem for this goal can be designed as the following. The objective is to minimize the deployment cost of the networks taking into account the costs of installing ANs and backhaul links connecting them to a central processor with specified capacities. The tentative constraints are:

- The probability that the net energy consumption per cell exceeds a given threshold has to be kept below a given parameter. The provided analysis in this paper can be used for the evaluation of this probability.
- All the machines should be able to successfully transmit their data on the designated time-slot. Since, the link capacity is a random variable there are possibilities that some machines require longer time slot for the transmission, which results in a time-slot overflow phenomenon. The designer has to guarantee that such events rarely happen by properly selecting the number of ANs.
- The designated capacity of the backhauls connecting ANs and central processors are limited. This may lead to the occasions that the accumulated traffic at an AN exceeds the corresponding backhaul's capacity. One may decide to increase the density of the ANs to reduce the traffic originating from the associated machines.

Our future investigations will comprehensively deal with these design problems.

V. Conclusions and Discussions

We borrowed tools from stochastic geometry and Poisson point process to model and study energy consumption in large-scale M2M communications by deriving the cumulative distribution function (CDF) of energy consumption. The transmission energy modeled in this paper was a function of transmission power, packet size, and link affordable capacity. We derived the laplace transform of the interference and then approximated it via log-normal distribution. We also calculated the Laplace transform of, and a lower bound on, the CDF

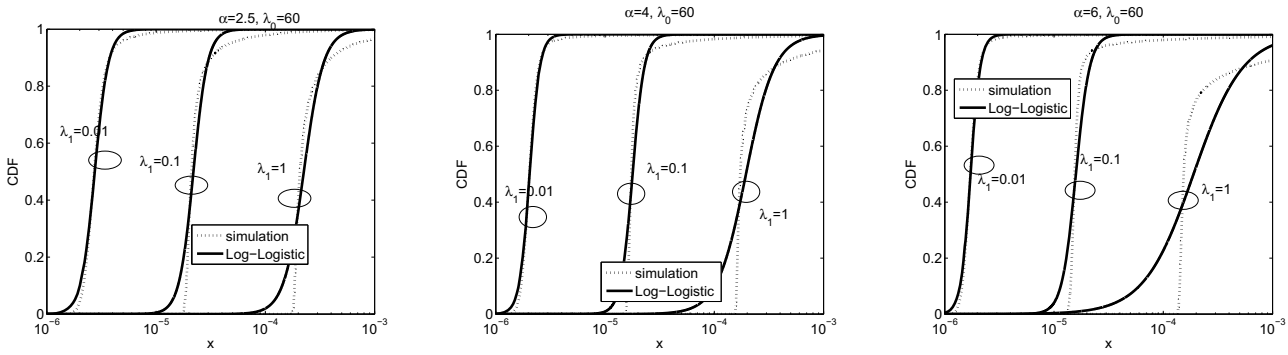

Fig. 4. CDF of the total energy consumption per cell with Log-Logistic Approximation.

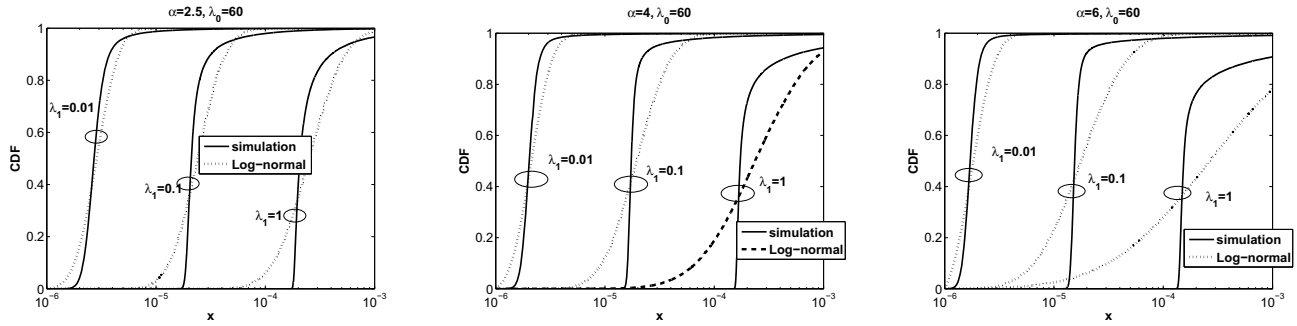

Fig. 5. CDF of the total energy consumption per cell with Log-Normal Approximation.

of the energy consumption in a cell. An empirical histogram revealed the suitability of the log-logistic distribution for approximating the CDF of energy consumption.

REFERENCES

[1] R. Lu, X. Li, X. Liang, X. Shen, and X. Lin, "GRS: The green, reliability, and security of emerging machine to machine communications," *IEEE Communications Magazine*, vol. 49, no. 4, pp. 28–35, April 2011.

[2] D. Niyato, L. Xiao, and P. Wang, "Machine-to-machine communications for home energy management system in smart grid," *IEEE Communications Magazine*, vol. 49, no. 4, pp. 53–59, April 2011.

[3] C. Y. Ho and C.-Y. Huang, "Energy-saving massive access control and resource allocation schemes for M2M communications in OFDMA cellular networks," *IEEE Wireless Comunications Letters*, vol. 1, no. 3, pp. 209–212, June 2012.

[4] H. Wu, C. Zhu, R. J. La, and Y. Z. X. Liu, "FASA: Accelerated S-ALOHA using access history for event-driven m2m communications," *IEEE/ACM Transactions on Networking*, 2013.

[5] J. Zhou, R. Q. Hu, and Y. Qian, "Scalable distributed communication architectures to support advanced metering infrastructure in smart grid," *IEEE Transactions on Parallel and Distributed Systems*, vol. 23, no. 9, pp. 1632–1642, September 2012.

[6] S. J. Baek and G. de Veciana, "Spatial model for energy burden balancing and data fusion in sensor networks detecting bursty events," *IEEE Transactions on Information Theory*, vol. 53, no. 10, pp. 3615–3628, October 2007.

[7] S. J. Baek, G. de Veciana, and X. Su, "Minimizing energy consumption in large-scale sensor networks through distributed data compression and hierarchical aggregation," *IEEE Journal on Selected Areas in Communications*, vol. 22, no. 6, pp. 1130–1140, August 2004.

[8] T. Kwon and J. M. Cioffi, "Random deployment of data collectors for serving randomly-located sensors," *IEEE Transactions on Wireless Communications*, 2013.

[9] T. Kwon and J.-W. Choi, "Multi-group random access resource allocation for M2M devices in multicell systems," *IEEE Communications Letters*, vol. 16, no. 6, pp. 834–837, June 2012.

[10] M. Haenggi, J. G. Andrews, F. Baccelli, O. Dousse, and M. Franceschetti, "Stochastic geometry and random graphs for the analysis and design of wireless networks," *IEEE Journal on Selected Areas in Communications*, vol. 27, no. 7, pp. 1029–1046, September 2009.

[11] F. Baccelli and S. Zuyev, "Poisson-voronoi spanning trees with application to the optimization of communication networks," *INRIA Research Report No. 3040*, November 1996.

[12] M. Z. Shafiq, L. Ji, A. X. Liu, J. Pang, and J. Wang, "Large-scale measurement and characterization of cellular machine-to-machine traffic," *IEEE/ACM Transactions on Networking*, 2013.

[13] Z. Hasan, H. Boostanimehr, and V. K. Bhargava, "Green cellular networks: a survey, some research issues and challenges," *IEEE Transactions Survey and Tutorials*, vol. 13, no. 4, pp. 524–540, Forth Quarter 2011.

[14] S. Foss and S. Zuyev, "On a certain voronoi aggregative process related to a bivariate poisson process," *Advanced in Applied Probability*, vol. 28, no. 4, December 1996.